Bulletin of Volcanology (2021) 83: 5
https://doi.org/10.1007/s00445-020-01429-w

RESEARCH ARTICLE

Volcanic facies as a guide to the palaeodepth and palaeotectonic setting of ancient oceanic crust: the case of the Nidar ophiolite, Ladakh, Indian Trans-Himalaya

Alok Kumar[1] · Hetu Sheth[2] · Prasenjit Barman[1,3] · Mohd Ibrahim[3]

Received: 17 July 2020 / Accepted: 16 December 2020 / Published online: 9 January 2021

Abstract

Ophiolites, found in orogenic belts, are slices of ancient oceanic lithosphere obducted on land during continental collision and ocean closure. They provide valuable insights into submarine volcanological and petrological processes. Palaeotectonic interpretations of ophiolites have heavily depended on geochemical data, despite the considerable submarine alteration and even metamorphism commonly observed in ophiolites. No independent checks on the geochemistry-based inferences are usually provided or sought. Here, we present a hitherto unavailable volcanic facies perspective on the ~ 140 Ma Nidar ophiolite, exposed > 4100 m above sea level in the Ladakh region of the Indian Trans-Himalaya. We describe features of pillow lavas and hyaloclastite forming the oceanic crust and of peperite and silicic volcanic ash layers in the overlying sedimentary cover (mainly radiolarian cherts, dated at 132–112 Ma). The whole volcanosedimentary sequence is inconsistent with a mid-ocean ridge setting. We interpret it as having formed in a shallow (~ 2.5 km) submarine environment, with ongoing explosive silicic eruptions, in an Early Cretaceous, compositionally bimodal, intra-oceanic island arc in the Neo-Tethys Ocean. Geochemical-isotopic data on the Nidar ophiolite have previously been used to argue for an intra-oceanic arc origin. We suggest that a volcanic facies approach to the study of ophiolites can be a valuable guide to their palaeodepths and palaeotectonic settings.

Keywords Oceanic crust · Pillow lava · Neo-Tethys · Ladakh · Trans-Himalaya · Nidar ophiolite

Introduction

Oceanic basalt is the most widespread terrestrial volcanic rock and occurs in a range of tectonic settings such as mid-ocean ridges, intraplate islands, oceanic plateaus, island arcs and back-arc basins (Batiza and White 2000; White et al. 2015; Perfit and Soule 2016). Volcanic processes currently forming new oceanic crust can be directly observed using devices such as manned submersibles. This has the advantages of being able to sample fresh and unaltered basalts and to map the areal distribution and surface morphology of the lavas, with both the eruption depth and tectonic setting well constrained (White et al. 2015). In contrast, neither eruption depth nor tectonic setting is directly known for ancient oceanic crust, preserved in ophiolites which are slices of obducted oceanic lithosphere found in continental orogenic belts (Coleman 1977; Dilek 2003). Both parameters are important for understanding the geological histories of orogenic belts and for plate tectonic reconstructions.

Basalt geochemistry and the so-called tectonic discrimination diagrams (e.g. Pearce and Cann 1971; Shervais 1982; Verma 2010; Dilek and Furnes 2011; Pearce 2014) have been the most widely used tools for inferring the palaeotectonic settings of ophiolites (e.g. Beccaluva et al. 1994; Ghazi et al. 2004; Kakar et al. 2014). However, considerable submarine hydrothermal alteration and even metamorphism (in the greenschist to amphibolite facies) are commonly seen in ophiolites. The primary chemical and isotopic compositions of the basalts, including abundances of even the relatively alteration-resistant elements (such as Nb, Zr and Ti), may have

Editorial responsibility: R.J. Brown

✉ Hetu Sheth
hcsheth@iitb.ac.in

[1] Centre of Advanced Study in Geology, Institute of Science, Banaras Hindu University (BHU), Varanasi 221005, India

[2] Department of Earth Sciences, Indian Institute of Technology Bombay, Powai, Mumbai 400076, India

[3] Geological Survey of India (GSI), Northern Region, Aliganj, Lucknow 226024, India

been significantly modified. Additionally, modern basalt lavas erupted in very different tectonic settings, specifically ocean island basalts and continental intraplate and rift basalts, have closely similar geochemical compositions (Fitton 2007; Sheth 2008). Geochemical plots proposed to serve as tectonic discrimination frequently do not achieve the purpose (Li et al. 2015), and Xia and Li (2019) emphasise that these diagrams cannot be used in isolation. Thus, it is arguable whether geochemical plots *can* indicate tectonic setting, because igneous rock compositions are strongly determined by sources and processes and not by tectonic setting (Rollinson 1993; Sheth et al. 2002).

Here, we ask whether volcanic facies can provide clues to the palaeodepth and palaeotectonic setting of an ophiolite, and serve as an independent check on geochemistry-based interpretations. Our chosen case study, the Nidar ophiolite, is exposed > 4100 m above mean sea level in the Ladakh region of the Indian Trans-Himalaya (Fig. 1). It is an ~ 8-km-thick sequence of ~ 140 Ma Neo-Tethyan oceanic lithosphere. Its mantle section is relatively well studied, but the volcanic section is poorly described. We describe the salient features of the volcanic section and discuss how the combined volcanological features are a guide to the environment of formation of this spectacular slice of oceanic lithosphere.

Regional geology

The Indus–Tsangpo suture of southern Tibet marks the collision zone between India and Asia (e.g. Gansser 1980; Virdi 1986; Thakur 1990). It is marked by several volcanic and ophiolite belts thought to represent intra-oceanic island arcs in the Neo-Tethys Ocean (e.g. Honegger et al. 1982; Dietrich et al. 1983; Aitchison et al. 2000). The westward extension of the Indus–Tsangpo suture into the Ladakh region of the Indian Trans-Himalaya is represented in the Dras, Spontang and Nidar ophiolites (Thakur and Misra 1984; Corfield et al. 2001; Mahéo et al. 2004) (Fig. 2).

The Nidar ophiolite, the focus of the present study, is exposed in southeastern Ladakh in a NW–SE-elongated outcrop (the regional structural trend of the Himalaya) just south of the Indus (Sindhu) River. The river flows along the suture between the Indian and the Asian plates (Fig. 2). Just north of the suture is the 110–50 Ma, calc-alkaline, Ladakh granite batholith and the Dras volcanic arc, which represent subduction of the Neo-Tethyan ocean floor under the Asian active continental margin, followed by the mid-Eocene India–Asia collision and underthrusting of the northern Indian continental margin under Asia (Honegger et al. 1982; Dietrich et al. 1983; Bhutani et al. 2004; Kumar et al. 2016). The Nidar ophiolite is thrust over the Zildat melange, which contains basalts, argillaceous rocks and "exotic" limestone blocks (Colchen 1999). South of the ophiolite and the melange, the ultrahigh-pressure Tso Morari gneisses and eclogites of the northern Indian continental margin are exposed, surrounded by the Mata unit composed of Palaeozoic, greenschist-facies metasedimentary rocks (Mukherjee and Sachan 2001; de Sigoyer et al. 2004). Further southwards, the Zanskar unit or Tethyan sequence is composed of Palaeozoic and Mesozoic continental shelf sediments of the northern Indian continental margin, and the Higher Himalayan crystallines represent Precambrian rocks of the Indian shield forming the central axis of the mountain range (Gansser 1964).

The ~ 8-km-thick Nidar ophiolite sequence consists of cherts, pillow lavas and gabbros (intruded by plagiogranite dykes) forming the crustal section, and peridotites constituting the mantle section (Thakur and Bhat 1983; Rameshwar Rao et al. 2004; Das et al. 2015; Buchs and Epard 2015, 2019). The ophiolite became highly dismembered during obduction, as pillow lavas of the ophiolite are also found at Mahe 20 km northwest of Nidar at 4178 m elevation, and halfway between Nyoma and Mahe at 4150 m (Fig. 2). There has been considerable interest in the mantle peridotites, which are

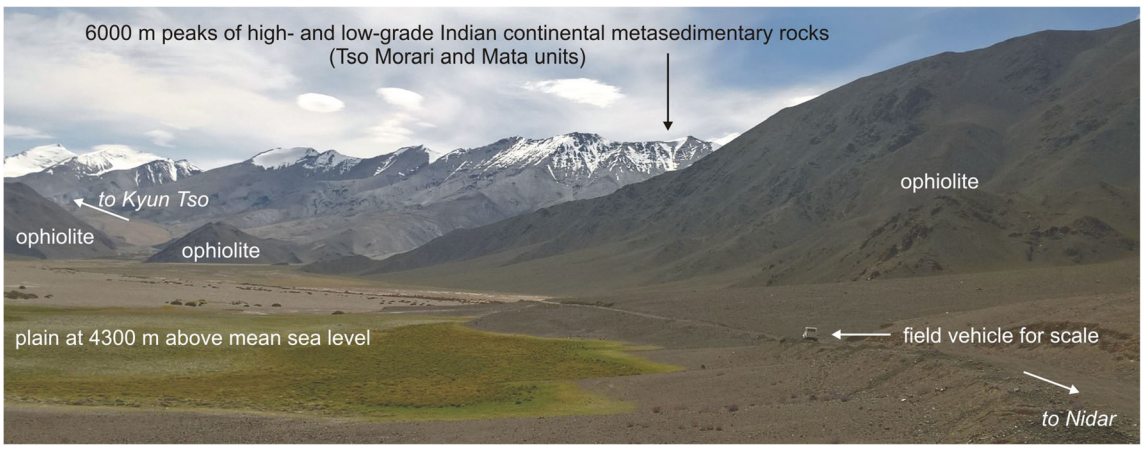

Fig. 1 Landscape of the Nidar ophiolite in summer (September 2019). View is approximately towards south

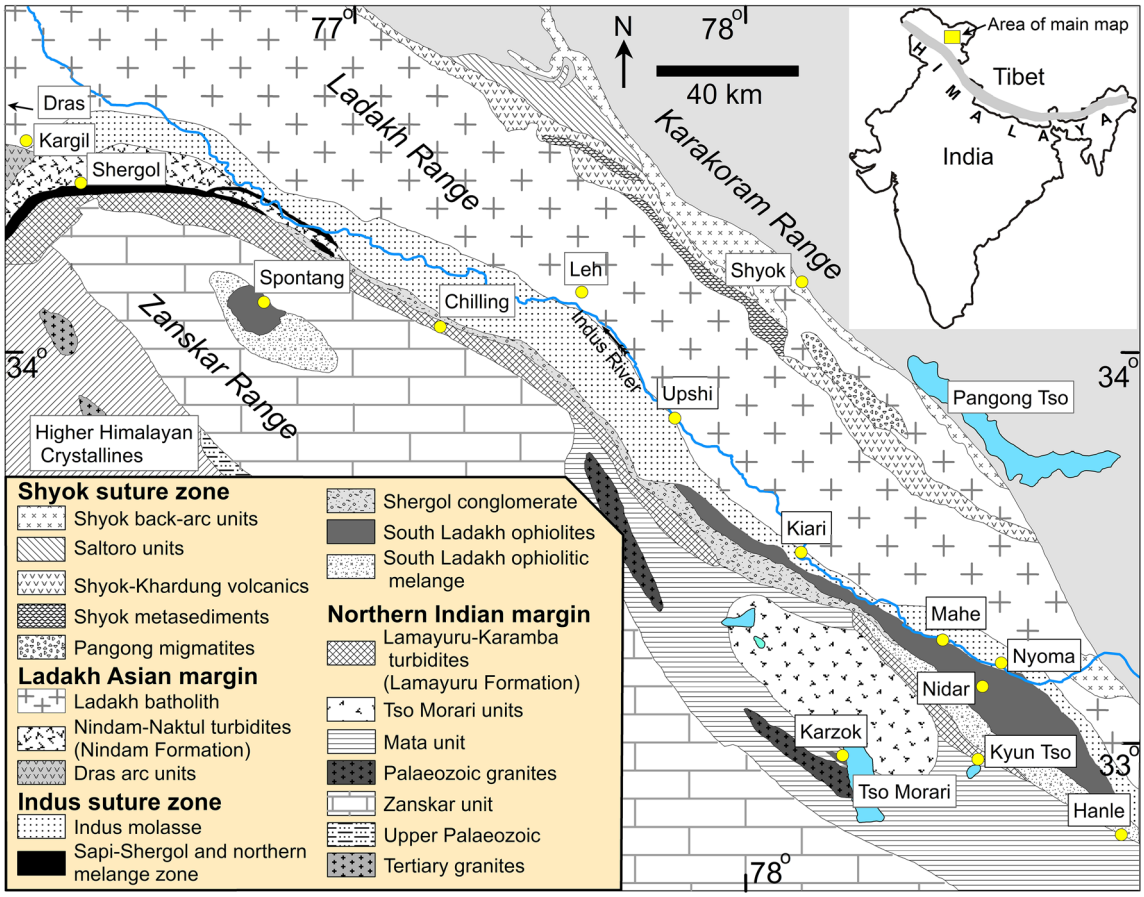

Fig. 2 (Inset) Map showing the Indian subcontinent, Tibet, and the Himalaya mountains in between, with the small box showing the part of the Ladakh region of the Indian Trans-Himalaya enlarged in the main figure. The main figure is a geological map of Ladakh, modified after Virdi (1986) and Mahéo et al. (2004), showing the major lithological and stratigraphic units and the localities mentioned in the text. In the map legend, the units are listed from north to south. The Indus River and various high-altitude lakes (including Kyun Tso, Tso Morari and Pangong Tso) are shown in blue

harzburgites and dunites, partly serpentinised and frequently chromite-bearing (e.g. Ravikant et al. 2004; Duraiswami et al. 2014; Das et al. 2015; Ray et al. 2017; Nayak and Maibam 2020). The gabbros have experienced ocean floor metamorphism to greenschist and amphibolite facies, and Mahéo et al. (2004) obtained $^{40}Ar/^{39}Ar$ cooling ages of 130–110 Ma on gabbros with metamorphic amphiboles. The basalts are also hydrothermally altered, and their vesicles are filled with chlorite, carbonates and quartz.

Linner et al. (2001) obtained a Sm–Nd isochron age of 140.5 ± 5.3 Ma on a Nidar gabbro, but this is only a two-point (plagioclase–clinopyroxene) isochron. Using Sr–Nd isotopic data on gabbros and basalts, they considered that the Nidar ophiolite formed in a marginal basin. Based on geochemical and Sr–Nd isotopic data for mafic and ultramafic rocks, Mahéo et al. (2004) and Ahmad et al. (2008) inferred a depleted mantle source metasomatised by subduction-derived fluids. Ahmad et al. (2008) obtained an imprecise mineral–whole rock Sm–Nd isochron age of 140 ± 32 Ma for the Nidar gabbros, whereas radiolarian cherts that form the sedimentary cover of the Nidar volcanic sequence have been dated biostratigraphically to 132–112 Ma (Thakur and Virdi 1979; Kojima et al. 2001; Zyabrev et al. 2008). These age constraints and geochemical arguments have led to the inference that the Nidar ophiolite represents a slice of Neo-Tethyan oceanic lithosphere ~140 Ma in age, and the Nidar ophiolite and the Spontang ophiolite to its northwest (Fig. 2) represent the crustal and mantle sections of an intra-oceanic island arc (Mahéo et al. 2004; Ahmad et al. 2008).

Field and petrographic observations

Pillow lavas

The Nidar ophiolite is best exposed around Nidar village, located 4216 m above sea level between the town of Nyoma and the lake of Kyun Tso (Figs. 1 and 2). Elongated exposures of pillow lavas are found on the mostly smooth, scree-covered slopes of linear mountain ridges around Nidar (Fig. 3a). Pillow size is variable (Fig. 3b). The larger pillows at Nidar

Fig. 3 **a**–**f** Photographs of pillow lavas and associated features of the Nidar ophiolite at Nidar village, with GPS coordinates N 33° 09′ 55.9″, E 78° 36′ 27.0″, elevation 4216 ± 3 m. **a** Typical summer landscape and pillow lava exposure. Geologists (encircled) for scale. **b** Cross section of the elongated pillow lava outcrop in **a**. Geologists for scale. White object above mound is a small religious construct. **c** Enlarged view of the pillows at the exposed base of the outcrop in **a** and **b**. **d** Highly vesicular pillow (centre) and small feeder tubes. Vertical face. Pen for scale is 15 cm long. **e** Feeder tubes in the pillow breccia in vertical section. **f** Feeder tubes and cross sections of numerous small pillows exposed in plan view. Pickhammer in **e** and **f** is 33 cm long

are ~ 1 m in diameter and are generally roughly spherical and bulbous with glassy surfaces (Fig. 3c, d). Pillow breccia is usually present between the pillows, and many small, filled feeder tubes are seen around the pillows and in the pillow breccia (Fig. 3e, f). Pillows exposed in cross section commonly depict a very fine-grained, highly vesicular interior with a glassy rind (Fig. 3d), and some pillows show radially arranged pipe vesicles along their marginal parts (Fig. 3f). A petrographic study of the Nidar pillow lavas shows that the glassy rinds are dominantly composed of spherulitic growths of plagioclase forming sheaf-like, bow-tie and fully radial patterns (Fig. 4a–c).

Basalt pillows of an elongate shape, and overlain by hyaloclastite (described below), are exposed 5 km southwest of Nidar village, at 4304 m elevation, on the road to Kyun Tso (Fig. 5a). These pillows have highly vesicular interiors with hundreds of tiny (≤ 1 mm) vesicles of subspherical shape, many of which have been filled by secondary calcite and zeolites (Fig. 5a–c). In some pillows, the vesicle concentration is markedly greater along the marginal parts just under the rind, compared to that in the pillow interior (Fig. 5b). Similarly, pillows with highly vesicular (now amygdaloidal) interiors, and vesicle-poor glassy rinds, are found in roadside boulders 10 km northwest of Nyoma on the way to Mahe, at 4150 m elevation (Fig. 5d–f).

At Mahe, pillow lavas form sections hundreds of meters thick (Fig. 6a). We observed a tumulus at road level with a characteristic domal shape (Fig. 6b). The overlying pillow lava sequence has abundant pillow breccia, and the pillows range in size from ~ 50 cm to only a few centimeters (Fig. 6c–e). Several pillows may lie juxtaposed, or an individual pillow may be enclosed in pillow breccia. Small, elongate, filled lava tubes traverse the pillow breccia (Fig. 6f). Some pillows evidently grew from these tubes into the surrounding breccia matrix, as shown by well-exposed necks (Fig. 6e).

The Mahe pillow lava sequence grades upwards into massive sheet lava (Fig. 7a, b) without a distinct eruptive break. The boundary between the pillowed and the massive

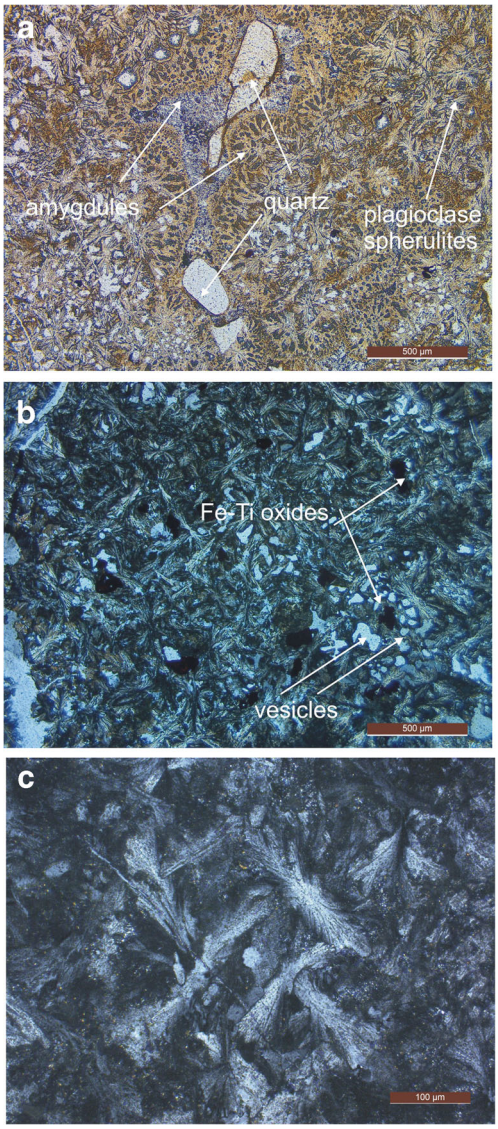

Fig. 4 **a**–**c** Thin-section photomicrographs of the glassy rinds of small pillows from Nidar village. Photomicrograph is **a** in plane polarised light and **b** and **c** in cross-polarised light. The views in **b** and **c** are dominated by plagioclase spherulites

types is irregular but subhorizontal (Fig. 7a, b). The sheet lava is many meters thick with its top eroded (Fig. 7c) and is intruded by a 5-m-wide dolerite dyke which shows blocky jointing and two distinct chilled margins (Fig. 7c, d).

Hyaloclastite

At the location 5 km southwest of Nidar village on the road to Kyun Tso (Figs. 2 and 5a), hyaloclastite is seen overlying a stack of elongate pillow lavas (Fig. 8a–d). The hyaloclastite contains innumerable angular fragments of relatively unaltered basalt that range in size from 1- or 2-cm- to decimeter-sized blocks, and more rarely blocks > 1 m in size, in a fine, sand- to clay-sized, grey to green matrix which is extensively altered from the original basalt (Fig. 8b, c). Parts of the hyaloclastite with the smaller basalt fragments show relatively well-developed centimeter-scale, ungraded bedding (Fig. 8c). In other parts of the same deposit, however, bedding is absent or is very crude at best, and many fragments and blocks of basalt are dispersed within a largely structureless and chaotic deposit (Fig. 8c, d). The ash-sized matrix contains millimeter- to centimeter-sized chips of basaltic glass (Fig. 8d). Small (centimeter-thick), subvertical, *en echelon* basaltic dykelets intrude the hyaloclastite. A petrographic study of the hyaloclastite matrix and one of the basalt blocks (Fig. 8e, f) shows abundant phenocrysts of plagioclase and clinopyroxene, and a few phenocrysts of olivine, in a very fine-grained groundmass containing numerous elongated plagioclase laths.

The sedimentary cover

Thick deposits of Early Cretaceous radiolarian chert, forming the sedimentary cover of the ophiolite, crop out around Nidar (Fig. 9a, b). The cherts have been dated biostratigraphically to the Hauterivian (132 ± 2 to 127 ± 1.6 Ma) to the Aptian (121 ± 1.4 to 112 ± 1.1 Ma) (Kojima et al. 2001; Zyabrev et al. 2008) and provide an upper limit to the age of the basaltic crust below. The chert sometimes shows a clear depositional contact with pillow lava (Fig. 9a). Strongly tilted and tightly folded chert layers near Nidar village enclose layers of soft, white, silicic volcanic ash (Fig. 9b, c). A petrographic study of the ash (Fig. 9d) shows numerous crystals of quartz and feldspar in a very fine-grained matrix in which it is difficult to identify additional features, but this is mainly a crystal tuff.

Also found in the vicinity is a deposit in which centimeter- to decimeter-sized globular clasts (rarely, angular fragments) of basalt are present within a matrix of sandstone which dominates the deposit (Fig. 10a–f). The contact of this deposit with the well-bedded cherts exposed nearby (Fig. 9a, b) is hidden under the widespread scree cover. In contrast to the cherts, the deposit is structureless and lacks bedding (Fig. 10a–f). A petrographic study of the sandstone host shows clasts of glassy, phyric basalt lava along with numerous rounded grains of quartz and feldspars, grains of highly fractured quartz, as well as clasts of volcanic rocks and sandstone (Fig. 11a–d), suggesting similarities to greywackes. Some of the larger clasts are composite, made up of numerous smaller rounded to angular grains (Fig. 11c, d).

Volcanological interpretations

Pillow lavas

Pillow lavas on the seafloor are emplaced in the same manner and at the same low effusion rates as small-scale compound

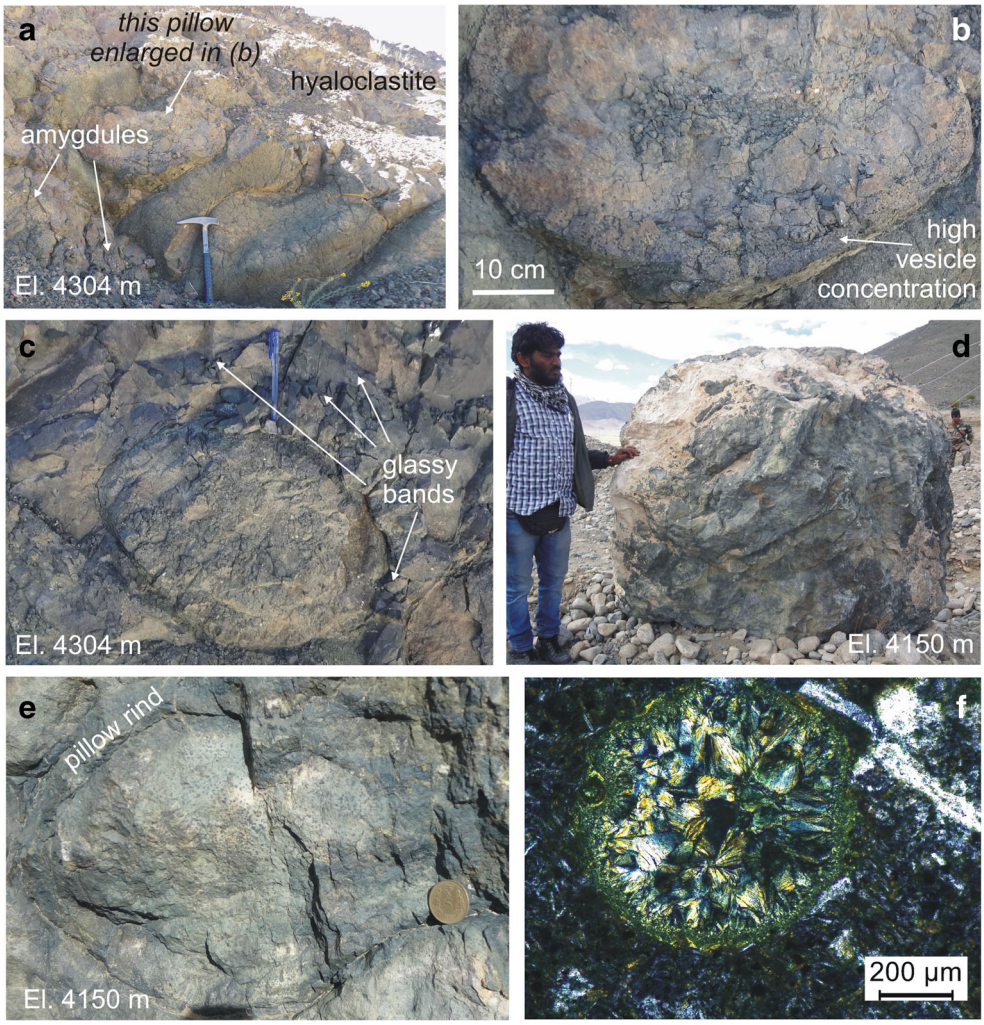

Fig. 5 **a** Elongate pillows underlying hyaloclastite, exposed 5 km southwest of Nidar village, on the eastern side of the road to Kyun Tso. Location N 33° 08′ 06.1″, E 78° 35′ 01.6″, elevation 4304 m. Vertical section, pickhammer is 33 cm long. **b**, **c** Highly vesicular basalt pillows (vertical section views) at the location in **a**. Pen in **c** is 15 cm long. **d** Highly weathered pillow lava forming roadside boulders 10 km northwest of Nyoma on the Nyoma–Mahe road. Location is N 33° 12′ 51.1″, E 78° 34′ 04.4″, 4150 m. **e** Highly vesicular–amygdaloidal and weathered basalt pillow in the boulder shown in **d**. Vertical face. The vesicles have been filled up by chlorite and other secondary minerals. Coin for scale is 2.5 cm wide. **f** Thin-section photomicrograph (in cross-polarised light) of an individual spherical amygdule in the pillow shown in **e**. The amygdule contains radial aggregates of secondary zeolite (stilbite). Note the fine grain size of the host basalt and veins of secondary minerals (white)

pāhoehoe flows of subaerial settings (e.g. Lewis 1914; Jones 1968; Moore 1975; Self et al. 1997; Duraiswami et al. 2013; Perfit and Soule 2016; Sheth 2018). The dominantly pillowed facies of the volcanic crust of the Nidar ophiolite thus indicates low eruption rates. Excellent evidence for their endogenous growth is provided by the numerous filled lava tubes (Fig. 3d–f) and the tumulus observed at the exposed base of the pillow lava section at Mahe (Fig. 6b). As in subaerial compound pāhoehoe flows, the tumulus, with its crust domed up, suggests localised inflation due to a feeder lava tube blocked downstream (e.g. Rossi and Gudmundsson 1996; Self et al. 1997; Duraiswami et al. 2001). The common occurrence of pillow breccia (Figs. 3e, f and 6c–f) indicates that individual pillows frequently tumbled down slopes under gravity and fragmented, as new pillows continued to form from tubes that carried fluid lava to different parts of a growing edifice in the manner of distributaries (e.g. Moore 1975; White et al. 2015; El Ghilani et al. 2017; Duraiswami et al. 2013, 2019). The abundant plagioclase spherulites in the chilled rinds of the pillows (Fig. 4a–c) attest to considerable undercooling of the lava in contact with cold seawater. As shown by Lofgren (1971, 1974), plagioclase crystal morphology is strongly dependent on the degree of undercooling ΔT, such that crystals are tabular at small ΔT and change to skeletal crystals, dendrites and spherulites with increasing ΔT.

Whereas eruption rates were generally low, they also locally increased greatly as reflected in the transition from pillow lava to thick sheet lava observed at Mahe (Fig. 7a–c). Submarine lobate or sheet flows (Batiza and White 2000; White et al. 2015; Perfit and Soule 2016) are not common in the Nidar ophiolite.

Submarine basalt lava does not extensively degas and vesiculate at considerable depths due to the high confining pressure, unless excessively volatile-rich, and in general, highly vesicular submarine basaltic lavas suggest a shallow (≤ 2 km) emplacement depth (e.g. Moore 1965; Jones 1969; Batiza and White 2000; White et al. 2015). Therefore, the highly vesicular nature of the pillows (Figs. 3d, 4a, b, and 5b, c, e, f) suggests a shallow (≤ 2 km) submarine setting for the Nidar ophiolite volcanic section.

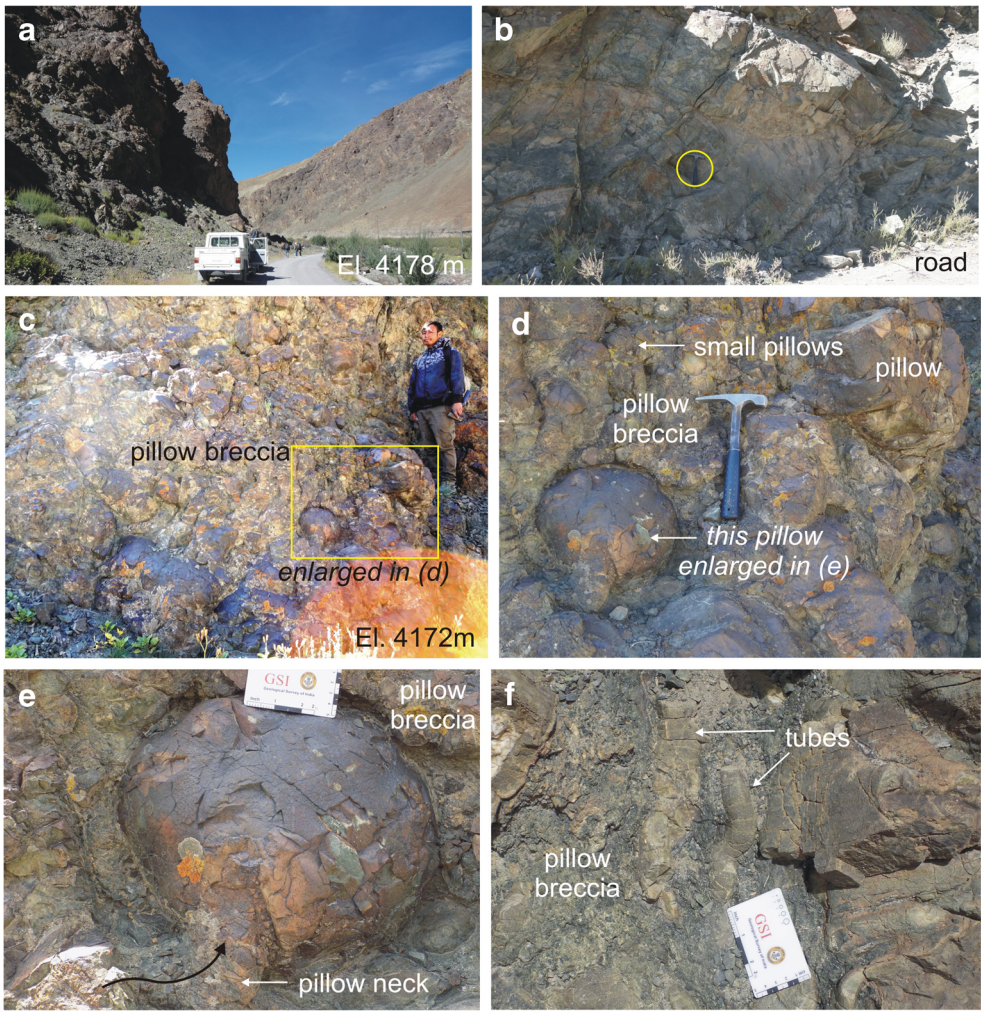

Fig. 6 **a**–**f** Photographs of pillow lavas and associated features of the Nidar ophiolite at Mahe, with GPS coordinates N 33° 15′ 40.0″, E 78° 27′ 10.0″, 4172 m. **a** Pillow lavas forming sections hundreds of meters thick. **b** Tumulus at the exposed base of the pillows. Vertical face. Pickhammer (encircled) is 33 cm long. **c** Numerous pillows of variable size enclosed in pillow breccia. Vertical face, person for scale. Photo has been edited on computer to enhance the contrast between pillows and breccia matrix. Bright orange patch of light in lower right results from the sun being in front of the camera. **d** Detail of the pillows and pillow breccia shown in **c**. **e** Close-up of a pillow surrounded by pillow breccia and connected by a neck to its feeder tube. Curved black arrow indicates the inferred direction of lava being fed into the pillow. Ruler is calibrated in inches (length 3 inches) and centimeters (width 5 cm). **f** Small feeder tubes in pillow breccia

Hyaloclastite

Hyaloclastite has not been described in the Nidar ophiolite so far, but it is known from other Tethyan ophiolites such as the ~95 Ma Andaman ophiolite (Jafri et al. 2010). Hyaloclastite is a clastic aggregate generated by the non-explosive quench fragmentation of hot basaltic lava in contact with cold seawater (Batiza and White 2000; White et al. 2015). The well-bedded hyaloclastite suggests quiet depositional conditions below wave base. The structureless and chaotic parts of the hyaloclastite indicate deposition by mass movements due to gravitational instabilities (rock falls and slides) or possibly even earthquakes, which disturbed any original bedding and brought large blocks of basalt (centimeters to over a meter in size) from shallower depths to greater depths. Hyaloclastite formation can occur at various depths, from shallow submarine conditions at emergent islands to deep submarine conditions in island arcs, mid-ocean ridges and seamounts (Batiza and White 2000).

Radiolarian chert

Radiolarian chert is a siliceous marine sedimentary rock commonly found overlying oceanic crust in ophiolites, and is often cited as indicating deep (~5 km) deposition (e.g. Holmes and Holmes 1978; Emiliani 1992; Tucker 2011). However, this aspect is complex and related to the concept of carbonate compensation depth (CCD). Briefly put, seawater contains increased amounts of dissolved CO_2 with depth as a combined effect of increasing pressure and decreasing temperature. Organic tests sinking through seawater, if composed of carbonate, begin getting dissolved as they cross the lysocline and are completely dissolved at the CCD, whereas siliceous tests (of radiolarians and diatoms) sink through the CCD unaffected. The CCD is thus the boundary between calcareous deposits above and non-calcareous deposits below and can be a guide to the palaeodepth of siliceous oceanic sediment such as that overlying the Nidar oceanic crust.

However, the CCD shows significant differences across the different oceans and with latitude even today, and has varied

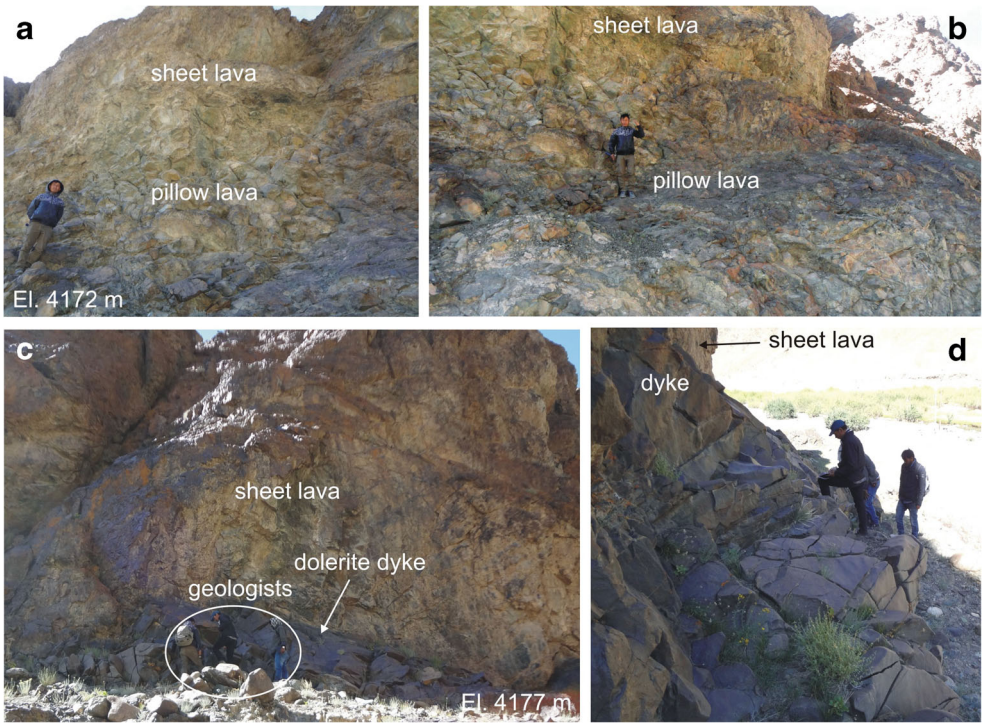

Fig. 7 **a**, **b** Pillow lava at Mahe grading upwards into massive sheet lava. Vertical section views, person for scale. Location is N 33° 15′ 40.0″, E 78° 27′ 10.0″, 4172 m. **c**, **d** Short, 5-m-thick dolerite dyke cutting sheet lava; geologists for scale, within ellipse in panel **c**. Dyke has an even texture in the interior and two distinct glassy chilled margins and strikes N 280° and dips steeply south. Location is N 33° 15′ 39.8″, E 78° 27′ 07.9″, 4177 m

greatly (several kilometers) through space and time (van Andel 1975; Thiede et al. 1980). It was shallow (around 3600 m) between the Late Jurassic and the early Late Cretaceous in the Pacific and Indian oceans (van Andel 1975). According to Sclater et al. (1977, cited in Thiede et al. 1980), the CCD in the Indian Ocean rose from an ~3500 m palaeodepth in the Late Jurassic to as shallow as 2.0–2.5 km palaeodepth by the mid-Cretaceous. This means that a CCD palaeodepth of 2.5–3 km may well apply to the 132–112 Ma Nidar radiolarian cherts deposited in the Neo-Tethys Ocean, implying their relatively shallow depth of deposition. The abundance of this Early Cretaceous radiolarian chert may also reflect the fact that carbonate-secreting pelagic microorganisms had evolved only shortly before, in mid-Mesozoic or Late Jurassic time (Tappan and Loeblich 1973; Saraswati and Srinivasan 2016). We therefore consider the bedded radiolarian cherts (Fig. 9a, b) overlying the Early Cretaceous Nidar oceanic crust as formed in a shallow submarine setting.

Peperite

We interpret the deposit containing globular basalt clasts in an impure sandstone matrix as a peperite. Peperite is a composite rock formed essentially in situ by the disintegration of magma which intrudes and mingles with unconsolidated or poorly consolidated, typically wet, sediment (Busby-Spera and White 1987; White et al. 2000; Skilling et al. 2002; El Desoky and Shahin 2020). The Nidar peperite thus suggests contemporaneous sedimentation and volcanism (or shallow-level intrusion).

Magma–sediment mingling is favoured when the intruding magma and the host wet sediment have similar densities and viscosities (Zimanowski and Büttner 2002). The mingling is aided by vapourisation of the pore waters by the heat of the magma and fluidisation of the sediment (Kokelaar 1982), and magma quenching and fragmentation of both rock types in a rheologically liquid-like or plastic condition (see Skilling et al. 2002 for a discussion of several other mechanisms). Cooling of the magma in a peperite occurs orders of magnitude slower than with water (White et al. 2015), but the poorly vesiculated basalt clasts in the Nidar peperite (Fig. 10c–f) suggest quenching before vesiculation could occur. The small glassy fragments in the sandstone matrix (Fig. 11a–c) reflect such quenching of juvenile basalt magma.

Magma–sediment mingling at Nidar also destroyed any former bedding. Peperites around the world are characteristically unstratified and ungraded and often highly discordant to bedding (White et al. 2000; Skilling et al. 2002). The Nidar peperite can be described as globular rather than blocky (terminology of Busby-Spera and White 1987; Skilling et al. 2002) and as dispersed rather than closely packed (terminology of Hanson and Wilson 1993). The exposed section of the peperite near Nidar village (Fig. 10a–f) does not show either a lava flow or an intrusion, but the intrusion was likely small and broke up entirely at the level observed.

Like the hyaloclastite, peperite has not been described in the Nidar ophiolite so far, but it is reported from other ophiolites such as the ~95 Ma Oman ophiolite (Jordan et al. 2008). Note that the 132–112 Ma age of the Nidar radiolarian cherts implies that the spatially associated dispersed peperite

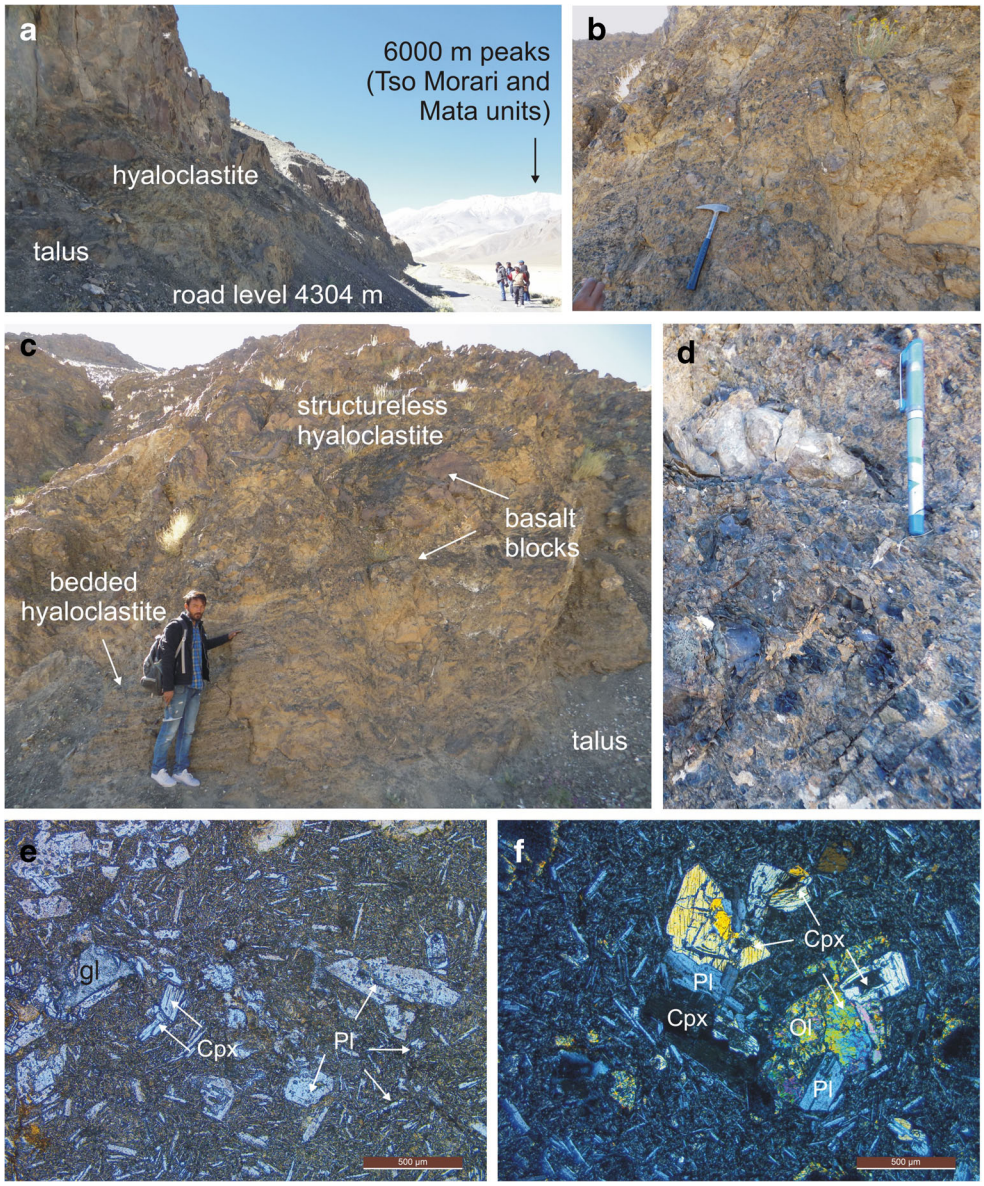

Fig. 8 **a**–**d** Photographs of hyaloclastite sequence in the Nidar ophiolite. Location is 5 km southwest of Nidar village on the eastern side of the Nidar–Kyun Tso road, at N 33° 08′ 06.1″, E 78° 35′ 01.6″, 4304 m. **a** 10-m-high cliff section of hyaloclastite. Geologists for scale. **b** Crudely bedded hyaloclastite with basalt blocks in a fine-grained ash-sized matrix. Vertical cliff face, pickhammer 33 cm long. **c** Well-bedded hyaloclastite (lower part of section) overlain by structureless hyaloclastite containing large basalt blocks. Person for scale. **d** Close-up (vertical face) of the hyaloclastite showing an irregularly shaped block of weathered basalt, and small angular chips of basaltic glass (tachylite) in a fine-grained ash-sized matrix. Pen is 15 cm long. **e** Thin section photomicrograph (in plane-polarised light) of the hyaloclastite, showing abundant plagioclase (Pl) forming phenocrysts and groundmass laths, and clinopyroxene (Cpx) crystals, some of which are indicated. "gl" is a glass shard. **f** Thin-section photomicrograph (in cross-polarised light) of one of the basalt blocks shown in panel **c**. The basalt contains abundant phenocrysts of Cpx (brilliant colours), fewer phenocrysts of Pl and a few phenocrysts of olivine (Ol, altered), in a fine-grained groundmass of the same minerals with abundant plagioclase laths

reflects small-scale, shallow-level, mafic intrusive activity continuing several million years after the formation of the underlying basaltic oceanic crust. The silicic ash layers found within the chert beds (Fig. 9b, c) indicate ongoing explosive eruptions at the same time. Below, we discuss the tectonic implications of all our combined observations and volcanological interpretations.

Discussion

Intermediate- and fast-spreading mid-ocean ridges, which have high magma supply rates, most commonly contain lobate and sheet flows, and hyaloclastite is rare or absent on fast-spreading ridges like the East Pacific Rise (Batiza and White 2000; White et al. 2015; Perfit and Soule 2016). The lack of

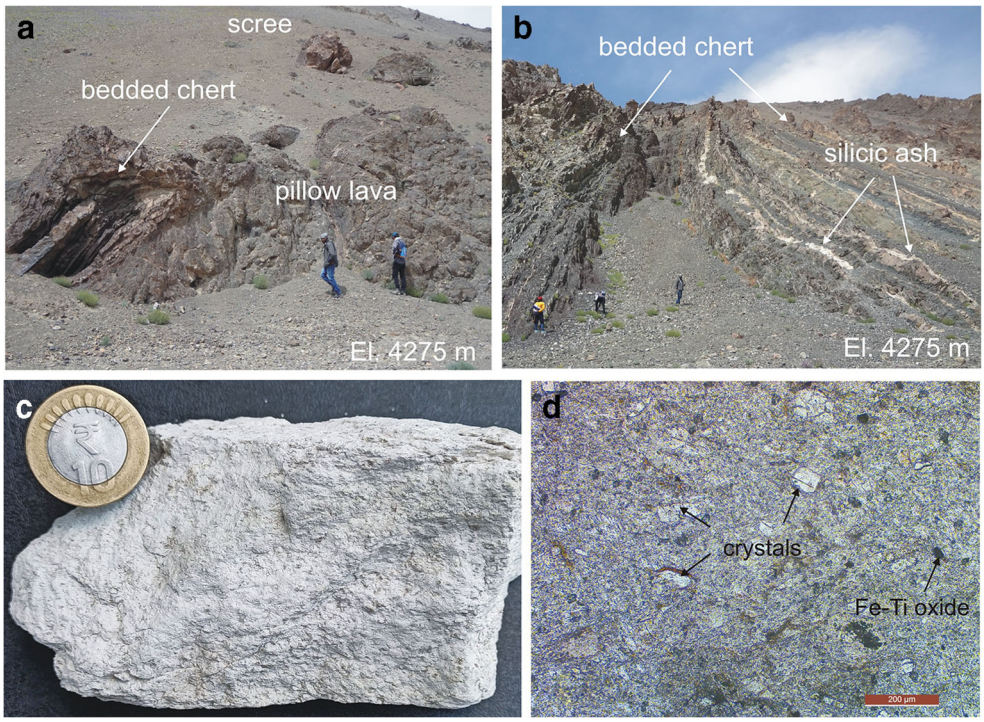

Fig. 9 **a** Bedded radiolarian cherts with a depositional contact above pillow lava, near Nidar village. Geologists for scale. **b** Thick, steeply inclined (75°–65°), N 330°-striking radiolarian chert sequence near Nidar village, enclosing layers of white silicic volcanic ash (two of which are indicated). Geologists for scale. Location N 33° 08′ 37.7″, E 78° 35′ 44.7″, 4275 m. **c** Close-up of the silicic ash. Coin for scale is 2.7 cm in diameter. **d** Thin-section photomicrograph of the ash (in plane-polarised light) containing abundant quartz and feldspar crystals (white) and a few Fe–Ti oxide grains (black), some of which are indicated

abundant sediment also characterises fast-spreading ridges. On the other hand, pillow lavas are the dominant lava type at slow-spreading ridges (which have low magma supply and lava extrusion rates) and on flanks of seamounts. These considerations rule out an origin of the Nidar ophiolite at an intermediate- to fast-spreading ridge. A slow-spreading ridge setting is also excluded by the fact that such ridges (such as the Mid-Atlantic Ridge) are deep-seated (Winter 2011, p. 264), whereas the abundantly vesicular pillow lavas require a shallow (≤ 2 km) emplacement depth, an explanation also favoured by the peperite which requires *unconsolidated* sediment to form.

Besides, the layers of soft silicic ash found in the chert cover (Fig. 9b, c) reflect explosive eruptions from distant or nearby volcanoes, and the abundant grains of quartz, feldspar and volcanic rocks in the sandstone matrix of the Nidar peperite suggest the input of terrigenous sediment from emergent land nearby. Several composite clasts (Fig. 11c, d) indicate that this sediment was reworked at least in part.

The simplest tectonic interpretation of the combined field and petrographic observations and volcanological interpretations is a mafic–silicic island arc, exemplified by modern intra-oceanic arcs such as the Kermadec, Mariana, or Andaman arcs (e.g. Kano 2003; Pal and Bhattacharya 2011; Saha et al. 2019). We suggest that the thick deposits of radiolarian chert in the Nidar ophiolite may themselves be a consequence of such a compositionally evolved island arc setting: erosion of the emergent silicic arc volcanoes would supply abundant SiO_2 to the sea, leading to proliferating biological (radiolarian) activity and ultimately extensive radiolarian chert deposition. Peperites are frequently associated with syn-volcanic intrusions in submarine sedimentary successions including those in island arcs (Hanson and Hargrove 1999; Gifkins et al. 2002).

Mahéo et al. (2004) and Ahmad et al. (2008) invoked an intra-oceanic arc setting for the Nidar ophiolite based on geochemical and isotopic data, which show no continental crustal signature but show the involvement of subduction-related fluids. That interpretation is consistent with the volcanological observations and interpretations we have made in the present study. The geochemical and volcanological interpretations complement and corroborate each other well in the case of the Nidar ophiolite. There can, however, be differences in detail. Ahmad et al. (2008) suggested that various arc-related magmatic rocks from the Indus suture zone contain a record of increasing arc maturity with time. According to them, the arc at 140 ± 32 Ma was immature and composed of mafic rocks, intermediate rocks (andesites and granodiorites) began forming at ~ 100 Ma, and finally rhyolites and diorites formed when India-Asia collision occurred at 50–45 Ma. However, the silicic ash layers in the 132–112 Ma radiolarian chert at Nidar village show that shallow-depth mafic intrusive activity (seen in the peperite) and explosive silicic eruptive activity were already occurring early on. Evolving arc maturity from mafic through intermediate to silicic compositions, over ~ 100 million years (Ahmad et al. 2008), is not in evidence.

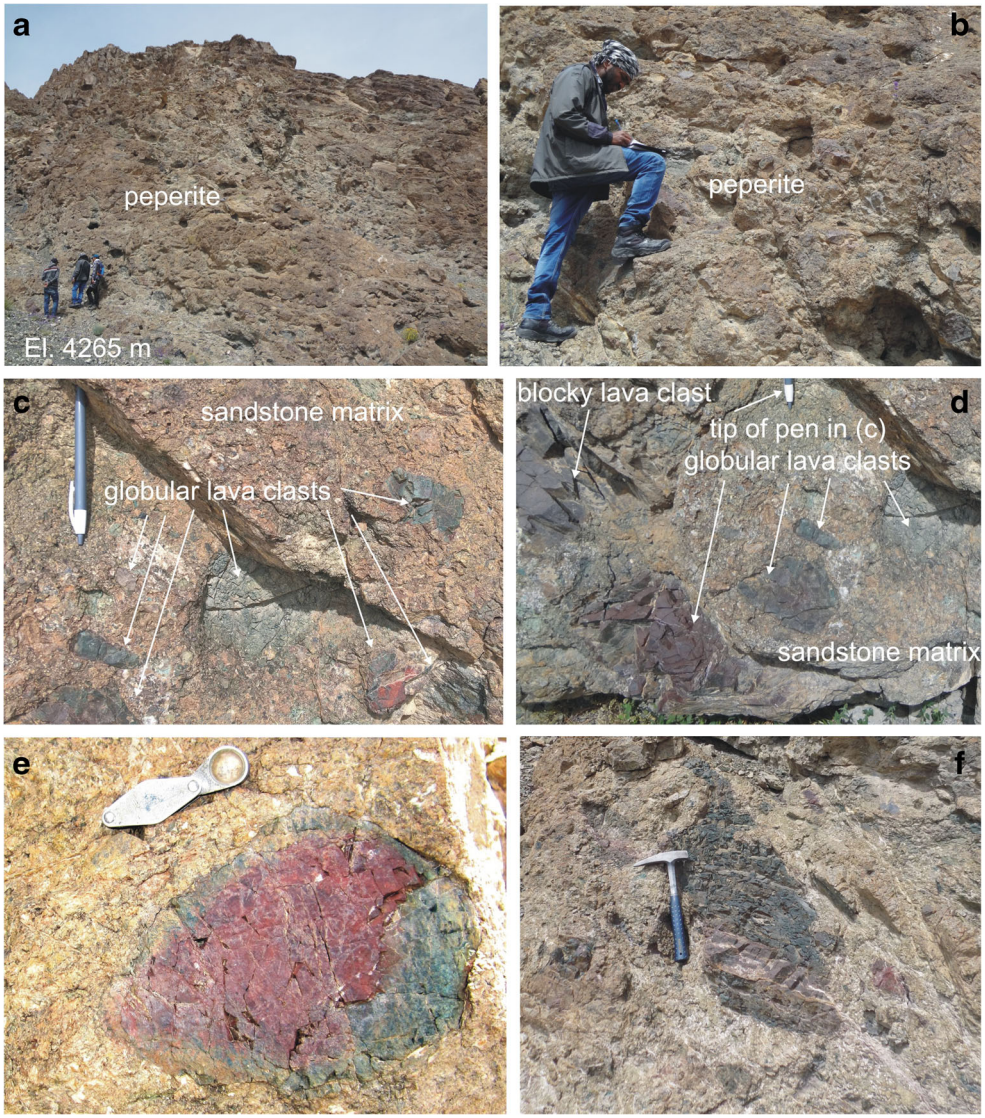

Fig. 10 **a**–**f** Outcrop of peperite near Nidar village, at location N 33° 08′ 39.8″, E 78° 35′ 55.7″, 4265 m. Geologists for scale in **a** and **b**. **c** Globular clasts of basalt in sandstone matrix. Vertical face, pen is 15 cm long. **d** Numerous globular basalt clasts and a blocky basalt clast with fractures in sandstone matrix. Vertical face. **e** Close-up of a globular basalt clast in chert matrix (vertical face); hand lens for scale. There are many tiny basaltic fragments in the matrix. **f** Large, irregularly shaped basaltic clast and several smaller ones in the chert matrix (vertical face). Pickhammer is 33 cm long

It is known that ophiolite sections commonly become tectonically dismembered during obduction on land (Coleman 1977), and such dismemberment has also affected the Nidar ophiolite. Around Nidar village, strong tectonic deformation is evident in the steeply to vertically dipping to tightly isoclinally folded radiolarian chert beds (Fig. 9b). It is curious therefore that a number of diverse field observations we have made in the Mahe section, such as the direction of convexity of the tumulus (Fig. 6b), the direction of convexity of the pillows (Fig. 6d, e) and the subhorizontal nature of the transition from pillowed lava to sheet lava (Fig. 7a, b), all suggest that this section is not only right side up, but the present horizontal is also roughly the palaeohorizontal. This, in turn, indicates only minor tectonic tilting of the obducted volcanic section. How this might have happened is a question for structural geologists, but it is possible that the Mahe section is the locally subhorizontal limb of a regional-scale fold whose steep to subvertical limb forms the Nidar village section.

Conclusions

The Early Cretaceous Nidar ophiolite in Ladakh, Indian Trans-Himalaya, is one of the important Tethyan ophiolites of the world. The basaltic volcanic facies in the Nidar ophiolite include abundant pillow lavas associated with hyaloclastite. Layers of silicic ash occur in the overlying radiolarian chert, and peperite is also found in the sedimentary cover. We interpret this assemblage to have formed in a shallow (2–2.5 km) submarine environment in

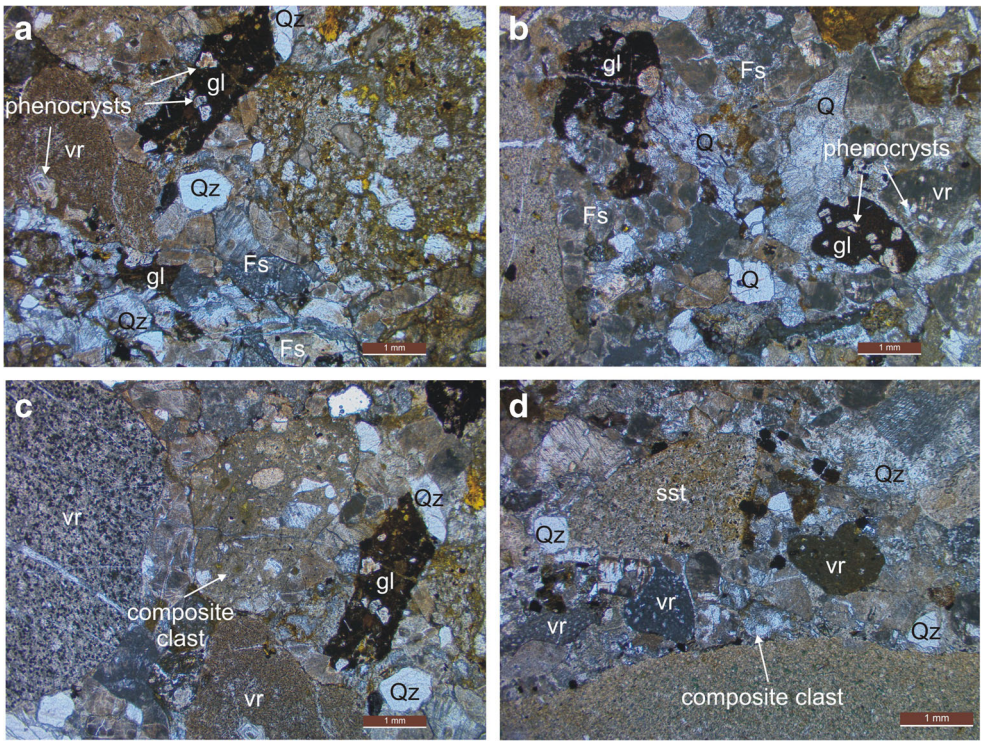

Fig. 11 **a**–**d** Thin section photomicrographs (in plane-polarised light) of the peperite matrix. The photomicrographs show glassy fragments (gl) showing quenched juvenile magma, besides grains of quartz (Qz), feldspars (Fs), sandstone (sst) and volcanic rocks (vr), some of which are indicated. Some of the phenocrysts present in the glass and volcanic rock fragments are indicated. Note composite clasts in panels **c** and **d**

a compositionally bimodal intra-oceanic island arc in the Neo-Tethys Ocean, consistent with past interpretations based on geochemical (including Sr–Nd isotopic) data. Geochemical data are very useful, in fact essential, in understanding the petrogenesis (mantle vs. crustal sources and magmatic processes) of ophiolites. However, palaeotectonic interpretations of ophiolites based on geochemical data should be backed by independent lines of evidence. As shown here with the case study of the Nidar ophiolite, volcanic facies, seriously underutilised in the ophiolite literature, are a valuable guide to the palaeodepths and palaeotectonic settings of ophiolites, and constitute an independent check on their geochemistry-based tectonic interpretations.

Acknowledgements Prasenjit Barman and Mohd Ibrahim express their gratitude to the Additional Director General and Head of Department, Geological Survey of India, Northern Region, Lucknow, for giving the opportunity to carry out their annual field programme in Ladakh. We thank the officials of the Public Works Department in Nyoma and Leh for logistical support, Mr. Rajan of Hotel Munshi Continental, Leh, for hospitality and support, and Rigzin and Tsewang for field assistance. We are grateful to James D. L. White and P. K. Saraswati for valuable discussions and publications. The manuscript was considerably improved by the constructive reviews of Martin Jutzeler, Isobel Yeo and the Associate Editor Richard J. Brown.

Funding Field work was supported by Research start-up seed grant no. F.30-470/2019 (Basic Scientific Research, BSR) dated 18/06/2019 (BHU project no. M-14/64) to Alok Kumar from the University Grants Commission (UGC).

References

Ahmad T, Tanaka T, Sachan HK, Asahara Y, Islam R, Khanna PP (2008) Geochemical and isotopic constraints on the age and origin of the Nidar ophiolitic complex, Ladakh, India: implications for the Neo-Tethyan subduction along the Indus suture zone. Tectonophysics 451:206–224

Aitchison JC, Badeng Z, Davisf AM, Liu J, Luo H, Malpas JG, McDermid IRC, Wu H, Zyabrev SV, Zhou M (2000) Remnants of a Cretaceous intra-oceanic subduction system within the Yarlung–Zangbo suture (southern Tibet). Earth Planet Sci Lett 183:231–244

Batiza R, White JDL (2000) Submarine lavas and hyaloclastite. In: Sigurdsson H et al (eds) Encyclopedia of volcanoes. Academic Press, New York, pp 361–381

Beccaluva L, Coltorti M, Premti I, Saccani E, Siena F, Zeda O (1994) Mid-ocean ridge and supra-subduction affinities in the ophiolitic belts from Albania. Ofioliti 19:77–96

Bhutani R, Pande K, Venkatesan TR (2004) Tectono-thermal evolution of the India-Asia collision zone based on ^{40}Ar-^{39}Ar thermochronology in Ladakh, India. Proc Ind Acad Sci (Earth Planet Sci) 114:737–754

Buchs N, Epard J-L (2015) The Nidar ophiolite and its surrounding units in the Indus Suture Zone (NW Himalaya, India): new field data and interpretations. 13th Swiss Geosci Mtg, Basel, 1–2

Buchs N, Epard J-L (2019) Geology of the eastern part of the Tso Morari nappe, the Nidar ophiolite and the surrounding tectonic units (NW Himalaya, India). J Maps 15:38–48

Busby-Spera CJ, White JDL (1987) Variation in peperite textures associated with differing host-sediment properties. Bull Volcanol 49: 765–775

Colchen M (1999) Ophiolitic melanges of the Ladakh Indus suture zone, a key to understanding the geodynamic evolution of the Indian and

Tibetan Tethyan margin. 14th Himalaya-Karakoram-Tibet Workshop, Tuebingen, Germany, Terra Nostra 99:28

Coleman RG (1977) Ophiolites. Springer, New York 220 p

Corfield RI, Searle MP, Pedersen RB (2001) Tectonic setting, origin, and obduction history of the Spontang ophiolite, Ladakh Himalaya, NW India. J Geol 109:715–736

Das S, Mukherjee BK, Basu AR, Sen K (2015) Peridotitic minerals of the Nidar ophiolite in the NW Himalaya: sourced from the depth of the mantle transition zone and above. In: Mukherjee S, Carosi R, van der Beek PA, Mukherjee BK, Robinson DM (eds) Tectonics of the Himalaya. Geol Soc Lond Spec Publ 412, 271–286

De Sigoyer J, Guillot S, Cosca M, Dick P (2004) Exhumation of the ultrahigh-pressure Tso Morari unit in eastern Ladakh (NW Himalaya): a case study. Tectonics 23:TC3003. https://doi.org/10.1029/2002TC001492

Dietrich VJ, Frank W, Honegger K (1983) A Jurassic-Cretaceous island arc in the Ladakh-Himalaya. J Volcanol Geotherm Res 18:405–433

Dilek Y (2003) Ophiolite concept and its evolution. In: Dilek Y, Newcomb S (eds) Ophiolite concept and the evolution of geological thought: Geol Soc Am Spec Pap 373:1–16

Dilek Y, Furnes H (2011) Ophiolite genesis and global tectonics: geochemical and tectonic fingerprinting of ancient oceanic lithosphere. Geol Soc Am Bull 123:387–411

Duraiswami RA, Bondre NR, Dole G, Phadnis VM, Kale VS (2001) Tumuli and associated features from the western Deccan volcanic province, India. Bull Volcanol 63:435–442

Duraiswami RA, Inamdar MM, Shaikh TN (2013) Emplacement of pillow lavas from the ~2.8 Ga Chitradurga greenstone belt, south India: a physical volcanological, morphometric and geochemical perspective. J Volcanol Geotherm Res 264:134–149

Duraiswami RA, Karmalkar NR, Kale MG, Sarkar PK, Shaikh TN, Jonnalagadda MK (2014) Pumpellyite-Yugawaralite aggregates in serpentinised harzburgite near Hanle, Nidar Ophiolite Belt, Ladakh Trans-Himalaya, India and their significance. Himal Geol 35:22–30

Duraiswami RA, Jutzeler M, Karve AV, Gadpallu P, Kale MG (2019) Subaqueous effusive and explosive phases of late Deccan volcanism: evidence from Mumbai Islands, India. Arab J Geosci 12:703. https://doi.org/10.1007/s12517-019-4877-z

El Desoky HM, Shahin TM (2020) Characteristics of lava-sediments interactions during emplacement of mid-Tertiary volcanism, Northeastern Desert, Egypt: field geology and geochemistry approach. Arab J Geosci 13:328. https://doi.org/10.1007/s12517-020-05310-0

El Ghilani S, Youbi N, Madeira J, Chellai EH, López-Galindo A, Martins L, Mata J (2017) Environmental implication of subaqueous lava flows from a continental large igneous province: examples from the Moroccan Central Atlantic Magmatic Province (CAMP). J Afr Earth Sci 127:211–221

Emiliani C (1992) Planet earth: cosmology, geology and the evolution of life and environment. Cambridge University Press, 736 p

Fitton JG (2007) The OIB paradox, in Fougler GR, Jurdy DM (eds) Plates, plumes and planetary processes. Geol Soc Am Spec Pap 430:387–409

Gansser A (1964) Geology of the Himalayas. Wiley InterScience, New York 289 p

Gansser A (1980) The significance of the Himalayan suture zone. Tectonophysics 62:37–52

Ghazi AM, Hassanipak AA, Mahoney JJ, Duncan RA (2004) Geochemical characteristics, ^{40}Ar-^{39}Ar ages and original tectonic setting of the Bande-Zeyarat/Dar Anar ophiolite, Makran accretionary prism. S E Iran Tectonophys 393:175–196

Gifkins CC, McPhie J, Allen RL (2002) Pumiceous peperite in ancient submarine volcanic successions. J Volcanol Geotherm Res 114:181–203

Hanson RE, Hargrove US (1999) Processes of magma/wet sediment interaction in a large-scale Jurassic andesitic peperite complex, northern Sierra Nevada, California. Bull Volcanol 60:610–626

Hanson RE, Wilson TJ (1993) Large-scale rhyolitic peperites (Jurassic, southern Chile). J Volcanol Geotherm Res 54:247–264

Holmes A, Holmes DL (1978) Principles of physical geology, 3rd edn. Halsted Press, New York 730 p

Honegger K, Dietrich V, Frank W, Gansser A, Thöni M, Trommsdorff V (1982) Magmatism and metamorphism in the Ladakh Himalayas (the Indus-Tsangpo suture zone). Earth Planet Sci Lett 60:253–292

Jafri SH, Sarma DS, Sheikh JM (2010) Hyaloclastites in pillow basalts, South Andaman Island, Bay of Bengal, India. Curr Sci 99:1825–1929

Jones GJ (1968) Pillow lava and pāhoehoe. J Geol 76:485–488

Jones GJ (1969) Pillow lavas as depth indicators. Am J Sci 267:181–186

Jordan BR, Fowler A-R, El Dein MB, El-Saiy AK, Abdelghanny O (2008) Peperites and associated pillow lavas subjacent to the Oman ophiolite. J Volcanol Geotherm Res 173:303–312

Kakar MI, Kerr AC, Mahmood K, Collins AS, Khan M, McDonald I (2014) Supra-subduction zone tectonic setting of the Muslim Bagh ophiolite, northwestern Pakistan: insights from geochemistry and petrology. Lithos 202–203:190–206

Kano K (2003) Subaqueous pumice eruptions and their products: a review. In: White JDL et al. (eds) Explosive subaqueous volcanism. Am Geophys Union Geophys Monogr 140, 213–230

Kojima S, Ahmad T, Tanaka T, Bagati TN, Mishra M, Kumar R, Islam R, Khanna PP (2001) Early Cretaceous radiolarians from the Indus suture zone, Ladakh, northern India. In: News of Osaka Micropal (NOM). Spec Vol 12:257–270

Kokelaar BP (1982) Fluidisation of wet sediments during the emplacement and cooling of various igneous bodies. J Geol Soc Lond 139:21–33

Kumar S, Bora S, Sharma UK (2016) Geological appraisal of Ladakh and Tirit granitoids in the Indus-Shyok suture zones of northwest Himalaya, India. J Geol Soc India 87:737–746

Lewis JV (1914) Origin of pillow lavas. Geol Soc Am Bull 25:591–654

Li C, Arndt NT, Tang Q, Ripley EM (2015) Trace element indiscrimination diagrams. Lithos 232:76–83

Linner M, Fuchs G, Koller F, Thöni M (2001) The Nidar ophiolite within the Indus suture zone in eastern Ladakh – a marginal basin ophiolite from the Jurassic-Cretaceous boundary. Abstract, 16th Himalaya-Tibet-Karakoram Workshop, Graz, Austria, J Asian Earth Sci 19:39

Lofgren G (1971) Spherulitic textures in glassy and crystalline rocks. J Geophys Res 76:5635–5648

Lofgren G (1974) An experimental study of plagioclase crystal morphology: isothermal crystallization. Am J Sci 274:243–273

Mahéo G, Bertrand H, Guillot S, Villa IM, Keller F, Capiez P (2004) The South Ladakh ophiolites (NW Himalaya, India): an intra-oceanic tholeiitic arc origin with implication for the closure of the Neo-Tethys. Chem Geol 203:273–303

Moore JG (1965) Petrology of deep sea basalt near Hawaii. Am J Sci 263:40–52

Moore JG (1975) Mechanism of formation of pillow lava. Am Sci 63:269–277

Mukherjee BK, Sachan HK (2001) Discovery of coesite from Indian Himalaya: a record of ultrahigh pressure metamorphism in Indian continental crust. Curr Sci 81:1358–1361

Nayak R, Maibam B (2020) Petrological study of spinel peridotites of Nidar ophiolite, Ladakh Himalaya, India. J Earth Syst Sci 129:47. https://doi.org/10.1007/s12040-019-1308-1

Pal T, Bhattacharya A (2011) Block-and-ash flow deposit of the Narcondam volcano: product of dacite-andesite dome collapse in the Burma-Java subduction complex. Island Arc 20:520–534

Pearce JA (2014) Immobile element fingerprinting of ophiolites. Elements 10:101–108

Pearce JA, Cann JR (1971) Ophiolite origin investigated by discriminant analysis using Ti, Zr and Y. Earth Planet Sci Lett 12:339–349

Perfit MR, Soule SA (2016) Submarine lava types. In: Harff J, Meschede M, Petersen S, Thiede J (eds) Encyclopedia of marine geosciences. Springer, 808–816

Rameshwar Rao DR, Rai H, Senthil Kumar J (2004) Origin of oceanic plagiogranite in the Nidar ophiolitic sequence of eastern Ladakh, India. Curr Sci 87:999–1005

Ravikant V, Pal T, Das D (2004) Chromites from the Nidar ophiolite and Karzok complex, Transhimalaya, eastern Ladakh: their magmatic evolution. J Asian Earth Sci 24:177–184

Ray D, Shukla AD, Bhattacharya S, Singh R, Nirmal Kumar T (2017) Serpentinite from Nidar ophiolite complex of Ladakh, India: implications for aqueous alteration to early Mars. Lunar Planet Sci XLVIII: 1935

Rollinson HR (1993) Using geochemical data: evaluation, presentation, interpretation. Longman Sci. & Tech, Essex 344 p

Rossi MJ, Gudmundsson A (1996) The morphology and formation of flow-lobe tumuli on Icelandic shield volcanoes. J Volcanol Geotherm Res 72:291–308

Saha AK, D'Mello NG, Sensarma S, Mudholkar AV, Kamesh Raju KA, Doley B (2019) Geochemical characteristics of submarine rhyolitic pumice from Andaman subduction zone: inferences on magmatism and tectonics of north-eastern Indian Ocean. Geol J 54:2779–2796

Saraswati PK, Srinivasan MS (2016) Micropalaeontology: principles and applications. Springer International Publishing Switzerland, 224 p

Sclater JG, Abbott D, Thiede J (1977) Palaeobathymetry and sediments of the Indian Ocean. In: Heirtzler J, Bolli HM, Davies TA, Saunders JB, Sclater JG (eds) Indian Ocean geology and biostratigraphy. Am Geophys Union Spec Publ 9:25–45

Self S, Thordarson T, Keszthelyi L (1997) Emplacement of continental flood basalt lava flows. In: Mahoney JJ, Coffin MF (eds) Large igneous provinces: continental, oceanic, and planetary flood volcanism. Am Geophys Union Geophys Monogr 100:381–410

Shervais JW (1982) Ti-V plots and the petrogenesis of modern and ophiolite lavas. Earth Planet Sci Lett 59:101–118

Sheth H (2008) Do major oxide tectonic discrimination diagrams work?: evaluating new log-ratio and discriminant-analysis-based diagrams with Indian Ocean mafic volcanics and Asian ophiolites. Terra Nova 20:229–236

Sheth H (2018) A photographic atlas of flood basalt volcanism. Springer, New York 363 p

Sheth HC, Torres-Alvarado IS, Verma SP (2002) What is the "calc-alkaline rock series"? Int Geol Rev 44:686–701

Skilling IP, White JDL, McPhie J (2002) Peperite: a review of magma-sediment mingling. J Volcanol Geotherm Res 114:1–17

Tappan H, Loeblich AR Jr (1973) Evolution of the oceanic plankton. Earth-Sci Rev 9:207–240

Thakur VC (1990) Indus Tsangpo suture zone in Ladakh – its tectonostratigraphy and tectonics. Proc Ind Acad Sci (Earth Planet Sci) 99:169–185

Thakur VC, Bhat MI (1983) Interpretation of tectonic environment of Nidar ophiolite: a geochemical approach. In: Thakur VC, Sharma KK (eds) Geology of Indus suture zone of Ladakh. Wadia Inst Him Geol, Dehradun, pp 21–31

Thakur VC, Misra DK (1984) Tectonic framework of Indus and Shyok suture zones in eastern Ladakh, northwest Himalaya. Tectonophysics 101:207–220

Thakur VC, Virdi NS (1979) Lithostratigraphy, structural framework, deformation, metamorphism of the SE region of Ladakh, Kashmir Himalaya. Himal Geol 22:46–50

Thiede J, Agdestein T, Strand JE (1980) Depth distribution of calcareous sediments in the Mesozoic and Cenozoic North Atlantic Ocean. Earth Planet Sci Lett 47:416–422

Tucker ME (2011) Sedimentary rocks in the field: a practical guide. Wiley Publ 288 p

Van Andel TH (1975) Mesozoic/Cenozoic calcite compensation depth and the global distribution of calcareous sediments. Earth Planet Sci Lett 26:187–194

Verma SP (2010) Statistical evaluation of bivariate, ternary and discriminant function tectonomagmatic discrimination diagrams. Turk J Earth Sci 19:185–238

Virdi NS (1986) Indus-Tsangpo suture in the Himalaya: crustal expression of a palaeo-subduction zone. Ann Soc Geol Pol 56:3–31

White JDL, McPhie J, Skilling I (2000) Peperite: a useful genetic term. Bull Volcanol 62:65–66

White JDL, McPhie J, Soule SA (2015) Submarine lavas and hyaloclastite. In: Sigurdsson H, Houghton B, Rymer H, Stix J (eds) The encyclopedia of volcanoes, 2nd edn. Academic Press, New York, pp 363–375

Winter JD (2011) Principles of igneous and metamorphic petrology, 2nd edn. Prentice-Hall 720 p

Xia L, Li X (2019) Basalt geochemistry as a diagnostic indicator of tectonic setting. Gondwana Res 65:63–67

Zimanowski B, Büttner R (2002) Dynamic mingling of magma and liquefied sediments. J Volcanol Geotherm Res 114:37–44

Zyabrev SV, Kojima S, Ahmad T (2008) Radiolarian biostratigraphic constraints on the generation of the Nidar ophiolite and the onset of Dras arc volcanism: tracing the evolution of the closing Tethys along the Indus-Yarlung-Tsangpo suture. Stratigraphy 5:99–112